

Black hole mass estimate in OJ 287 based on the bulk-motion comptonization model

Sergey Kuznetsov^{1*} & Lev Titarchuk²

¹*Prosto Science AI Lab, Montreal, QC, H2X 3X2, Canada*

²*Dipartimento di Fisica, Università di Ferrara, via Saragat 1, 44122 Ferrara, Italy*

Last updated 2024 February 5; in original form 2023 January 24

ABSTRACT

The multi-wavelength outburst activity in the BL Lacertae source OJ 287 has sparked a lot of controversy about whether the source contains one or two black holes (BHs) and what characteristics of this black hole binary would be. In this article we present the results of analysis of the X-ray flaring activity of OJ 287 using the data of *Swift*/XRT observations. We discovered that the energy spectra in all spectral states can be adequately fit with the XSPEC BMC model (the Comptonization one). As a result we found that the X-ray photon index of the BMC model, Γ correlates with the mass accretion rate, \dot{M} . We found the photon index Γ to increase monotonically with accretion rate \dot{M} from $\Gamma \sim 2$ in the intermediate state (IS) to $\Gamma \sim 2.5$ the high/soft state (HSS) with subsequent saturation at $\Gamma \sim 2.6$ level at higher luminosities. This type of behavior of the spectral index is remarkably similar to the pattern observed in a number of established stellar-mass black hole candidates. Assuming the universality of the observed pattern of the correlation between the photon index and mass accretion rate, we estimate the BH mass in OJ 287 to be around 2×10^8 solar masses, using the well studied BH binaries GX 339–4 and XTE J1859–226 to calibrate the model.

Key words: black hole physics—BL Lacertae objects:individual:OJ 287—galaxies:active

1 INTRODUCTION

The primary goal of our paper is to examine the value of the secondary black hole (BH) mass in OJ 287 applying the scaling method of BH mass determination [Shaposhnikov & Titarchuk (2009), hereafter ST09]. OJ 287 demonstrated a noticeable 12 yr cycle [Valtonen et al. (2006)] that can be explained by the presence of the accreting black hole binary system (BHBS) with systematic disturbance of the accretion disk (AD) around the primary by the secondary.

Valtonen et al. (2012), hereafter V12, presented results of the two X-ray observations of OJ 287 by *XMM-Newton* on April 12 and November 3–4, 2005. In Fig. 2 they plotted the observations of the 2005 campaigns. V12 claimed that for the April 12, 2005 the spectral energy distribution (SED), the spectrum from radio to X-rays followed nicely a synchrotron self-Compton (SSC) model. V12 further stated that the BH mass value of the secondary determined from the orbit solution $M_{sec} \sim 1.4 \times 10^8 M_{\odot}$ agrees with the measured properties of the optical outburst. V12 also formulated a question regarding the primary BH mass necessary to guarantee the stability of the primary accretion disc. They found that the minimum value of the primary mass $1.8 \times 10^{10} M_{\odot}$ is quite close to the BH mass determined from the orbit, $1.84 \times 10^{10} M_{\odot}$.

To find evidence for the emission of the secondary, V12 needed to look at the short time-scale variability in OJ 287. It has been found to be variable from 15 min time-scale upwards on many occasions [see for example, Gupta et al. (2012)] and on one occasion the light curve has shown sinusoidal variations with a period of 228 min (Sagar et al. 2004). If this variation is associated with the last stable

orbit of a maximally rotating black hole, the mass of the black hole would be $1.46 \times 10^8 M_{\odot}$ (Gupta et al. 2012), i.e. identical to the mass obtained from the orbit solution (Valtonen et al. 2010).

Komossa et al. (2021), hereafter KOM21 made a detailed analysis of *XMM-Newton* spectra of OJ 287 spread over 15 years. KOM21 also presented data from *Swift* UVOT and XRT observations of OJ 287, which began in 2015, along with all public *Swift* information after 2005. During this period, OJ 287 was found in the low/hard extreme state and outburst soft states. In addition, they established that the OJ 287 X-ray spectrum was highly variable, passing all states seen in blazars from the low/hard (flat) state to exceptionally soft steep state (ST). KOM21 found that these spectra can consist of two parts: IC radiation which is prevailing at the low-state, and very soft radiation component that becomes extremely powerful when OJ 287 becomes more luminous. KOM21 have concluded that their 2018 *XMM-Newton* spectra almost identical with the EHT examination of OJ 287, and were well characterized by a model with a hard IC component of the photon index $\Gamma \sim 1.5$ and a soft component.

We reanalyzed the data of the X-ray telescope (XRT) onboard of *Swift* Observatory for OJ 287 and applied the ST09 scaling method to this data in order to make a BH mass estimate. Using this method requires an accurate knowledge of the distance to the source OJ 287. The method was proposed back in 2007 by Shaposhnikov & Titarchuk (2007), hereafter ST07 and also by ST09. It is worth noting that there are two scaling methods: the first method based on the correlation between the photon index Γ and the quasi-periodic oscillation frequency (QPO) ν_L ; and the second method is based on the correlation between Γ and normalization of the spectrum proportional to \dot{M} . If the first method ($\Gamma - \nu_L$) is used to estimate the mass of the BH, the distance to the source is not required (ST07),

* E-mail: astro@prosto.science (SK)

but for the second method ($\Gamma - \dot{M}$) the source distance and the inclination of the accretion disk relative to the Earth observer are needed (ST09).

For both methods, it is important that the source shows a change in spectral states during the outburst and a characteristic behavior of Γ , namely, a monotonic increase of Γ with v_L or \dot{M} in the LHS→IS→HSS transition and reaching a constant level (saturating) at high values of v_L or \dot{M} , followed by a monotonic decrease in Γ during the HSS→IS→LHS transition during the outburst decay.

The saturation of Γ (so-called “ Γ -saturation phase”) during the outburst is a specific signature that this particular object contains a BH (Titarchuk & Zannias 1998). Indeed, the Γ -saturation phase can be caused only by an accretion flow converging to the event horizon of a BH [see the Monte-Carlo simulation results in Laurent & Titarchuk (1999, 2011)]. Because of this, it makes sense to compare BH sources that have the same Γ -saturation levels. In the second method ($\Gamma - \dot{M}$), it is assumed that BH luminosity is directly proportional to \dot{M} (and, consequently, to the mass of the central BH), and inversely proportional to the squared distance to the source. Thus, we can determine the BH mass by comparing the corresponding track $\Gamma - \dot{M}$ for a pair of sources with BHs, in which all parameters are known for one source, and for the other source parameters except a BH mass are known (for more details on the scaling method, see ST09).

The scaling method has a number of advantages in determination of a BH mass compared to other methods, namely, the calculation of the X-ray spectrum originating in the innermost part of disk based on first-principle (fundamental) physical models, taking into account the Comptonization of the soft disk photons by hot electrons of the internal disk part and in a converging flow to BH.

It is necessary to emphasize that our approach is only justifiable if the observed X-ray emission in OJ 287 is indeed produced by BMC in the accretion flow. In reality, it may be dominated by emission produced in relativistic jets, which is a popular explanation of the multi-wavelength emission properties of blazars in general. Nevertheless, we apply the scaling method to OJ 287 because, as will be shown below, it yields results (specifically, the spectral slope vs. normalization dependence) that indicate that at least a significant fraction of the observed X-ray emission in this blazar is produced by the BMC mechanism.

In this paper, based on *Swift* data analysis, we estimate a BH mass in OJ 287 by applying the scaling technique. In §2 we provide details of our data analysis while in §3 we present a description of the spectral models used for fitting of this data. In §4 we focus on observational results and their interpretation. In §5 we discuss the main results of the paper. In §6 we present our final conclusions.

2 OBSERVATION AND DATA REDUCTION

We analyzed observational data of OJ 287 carried out by XRT instrument aboard *Swift* observatory from April 2016 to June 2017 (MJD 57501-57918). We processed ~140 ks of pointed observations of the source. We retrieved the data from the UK *Swift* Science Data Centre Archive¹ and used XRT data both in Windowed Timing (WT) and Photon Counting (PC) modes.

The lowest source count rate was detected at the very beginning and at the end of this observational cycle (April–June 2016, May–June 2017). It corresponds approximately to XRT observations in PC

mode with the flux below ~1 mCrab. This covers 31 PC observations of ~34 ks in total. The rest of the observations were carried out during an epoch of strong flaring activity of OJ 287 in the middle of this period from October 2016 to April 2017 and they consisted of ~105 ks of 109 WT observations. We excluded only 3 very short observations from our analysis with accumulation time less than 100 s per ObsID and an additional 6 ones when the source position on the detector was at the edge of the field of view (FOV).

For our comprehensive analysis we reprocessed original Level 1 XRT data using standard `xrtpipeline` screening settings from HEASOFT package v6.30 and calibration files version 20210915. We also checked PC data for the pile-up effect and found its possible presence in 2 observations with contamination radius of 2 detector pixels.

The source spectra were extracted from every individual PC and WT observations for our preliminary analysis. For the PC mode we used a 30-pixel circular region for the source spectrum and a 60-pixel circular region taken from source-free area for background correction. Because of the lack of 2D-image in WT mode, we used a rectangular 20x40 pixels region co-aligned to the axis of 1D-image for both source and background spectra.

A typical pointed XRT observation of OJ 287 consists of ~1 ks or less. As such, a short duration did not allow us to obtain statistically significant best-fit spectral model parameters. At the same time, the estimation of the source flux by the applicable model to the spectrum can be a tool for the further averaging of individual source spectra over the flux. In order to implement this approach we used the `tbabs*bmc` (Bulk motion Comptonization) model with fixed $N_H = 2.7 \times 10^{20}$ and $\log(A) = 2.0$. The applicable above absorption toward OJ 287 was adopted from Willingale et al. (2013)² and constant $\log(A)$ was used for simplification and reduction of free model parameters.

The preliminary spectral analysis demonstrated the 0.3–10 keV source flux variations in the following ranges: $0.5\text{--}2.6 \times 10^{-11}$ and $0.5\text{--}4.1 \times 10^{-11}$ erg s⁻¹ cm⁻² for PC and WT observations. Since our goal was the averaging of the source spectra with similar flux, we grouped 31 PC and 100 WT observations into 7 and 18 flux bins correspondingly.

The procedure of retrieving averaged spectrum is trivial for PC observations and includes the following steps: reading of re-processed event files, application of region filters for source and background spectra extraction with `xselect`; building the accumulated exposure map with `ximage`; and generation of Ancillary Response Files (ARFs) with `xrtmkarf`. Similar to the preliminary spectral analysis described above per individual ObsID, we applied the same 30/60-pixel circular regions for the source extraction and background correction.

The retrieving of averaged source spectrum over WT observations is not trivial if the orientation of the detector does not match among all observations plus if the source positions on the detector were shifted. As a result, the averaged 2D-image will be a combination of 1D-images of the same length under different angles and with different shifts centered to the source position. The hardest task in this procedure is the proper background extraction and source/background area correction using event lists and builded exposure maps.

In order to extract the source spectrum from the set of accumulated WT observations, we used a 20-pixel circular region as a filter with `xselect`. In this case we extracted the source counts using the same 40-pixel width/length region as we did before for individual WT observations (see above). For background extraction we used the

¹ <https://www.swift.ac.uk/archive>

² <https://www.swift.ac.uk/analysis/nhtot>

Table 1. Parameters of scaling patterns of Eq. (1) for reference and target sources

Source	A	B	N_{tr}	β
XTE J1859-226	2.55	1.25	7.13E-2	1.00
GX 339-4	2.46	0.955	1.28E-1	1.60
OJ 287	2.54	0.42	1.33E-4	2.28

annulus centered to the source position with inner/outer radii of 80/120 pixels. Since the detector size is only 200 pixels in width, we are then getting the same 40 linear pixels of 1D-image on the detector despite the individual 1D-images orientations and shifts. The last step in getting of WT averaged spectrum is the manual correction of the background scaling factor stored in BACKSCAL keyword of the spectral file. Since the obtained background effective surface is actually the length and it has the same width of 40-pixels as the source, we then manually matched this value of BACKSCAL keyword in the header of the background file to the source spectrum one.

3 ANALYSIS AND RESULTS

For our comprehensive spectral analysis we fitted 7 PC and 18 WT averaged over the flux spectra by `tbabs*bmc` model with fixed $N_H = 2.7 \times 10^{20}$ (see above). The typical OJ 287 spectra with $\Gamma = 2.0$ and $\Gamma = 2.6$ are shown in Fig. 1.

For our further analysis we plotted the spectral index Γ vs N in Fig. 2. The correlation between Γ and N is noticeable for N lower than $\sim 2.5 \times 10^{-4}$. Taking into account that Γ does not fluctuate significantly at higher N values, we separated our data points shown in Fig. 2 in two parts and fitted them by linear function and a constant at lower and higher N correspondingly. The result of this best-fit approximation is shown in Fig. 2 by a solid line.

Additionally, we fitted the same data points using the analytic function

$$F(N) = A - B \ln \left[\exp \left(1.0 - (N/N_{tr})^\beta \right) + 1 \right] \quad (1)$$

widely used as scalable pattern between reference and target sources in black hole mass estimation (see ST09). The results of this approximation are shown in Table 1. GX 339-4 best-fit parameters corresponding to observed LHS to IS source transition in 2007 were taken from ST09 Fig. 3 and Table 2 (28 data points, online extended table). XTE J1859-226 data were adopted from ST09 (see Fig. 9 there).

Taking into account $F(N)$ tends asymptotically to a constant at infinity, we projected the saturation value of N we found for OJ 287 to $F(N)$. In Fig. 2 it corresponds to the projection of the break point of the solid curve to the dotted curve. We then repeated the same approach in scaling $F(N)$ for GX 339-4 and XTE J1859-226. For the reference sources N should be the same way equidistant from the upper limit of $F(N)$ as N for the target source. In other words, the relative height of N position between the asymptotes should be the same.

The curves corresponding to analytical function $F(N)$ of the reference and target sources from Table 1 and their N_t and N_r are shown in Fig. 3 in details.

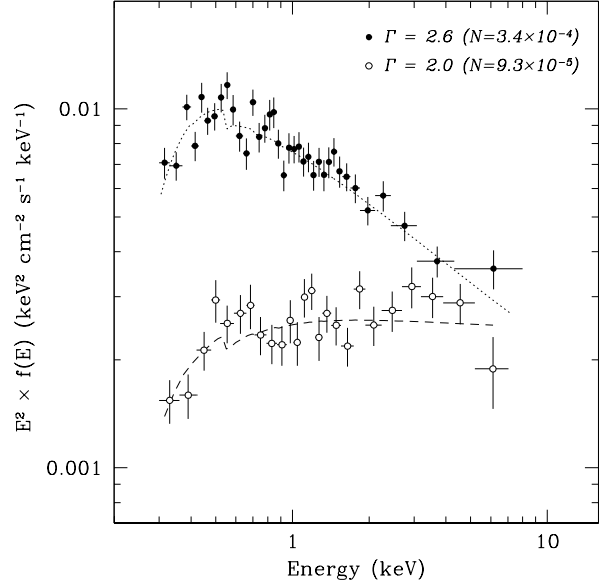


Figure 1. X-ray observed spectra of OJ 287, using the `tbabs*bmc` fit model for the high/soft (dotted line) and intermediate (dashed line) states. Spectra are presented as $E^2 f(E)$ -diagram where $f(E)$ is a photon spectrum. It is evident using this plot that the high/soft luminosity is at least four times higher than that in the intermediate state.

3.1 X-ray spectra

To fit the energy spectra of this source we used a XSPEC model consisting of the Comptonization (bulk-motion Comptonization, hereafter BMC) component [see Titarchuk & Zannias (1998); Laurent & Titarchuk (1999)]. We also used a multiplicative `tbabs` model (Wilms et al. 2000) which takes into account absorption by neutral material. We assume that accretion onto a BH is described by two main zones [see, for example, Fig. 1 in Titarchuk & Seifina (2021)]: a geometrically thin accretion disk [e.g. the standard Shakura-Sunyaev disk, see Shakura & Sunyaev (1973) and a transition layer (TL), which is an intermediate link between the accretion disk, and a converging (bulk) region (see Titarchuk & Fiorito (2004)], that is assumed to exist, at least, below 3 Schwarzschild radii, $3R_S = 6GM_{BH}/c^2$. The spectral model parameters are the equivalent hydrogen absorption column density N_H ; the photon index Γ ; $\log(A)$ is related to the Comptonized factor $f [= A/(1+A)]$; the color temperature and normalization of the seed photon blackbody component, kT_s and N , respectively.

Similarly to the ordinary `bbody` XSPEC model, normalization is a ratio of the source (disk) luminosity L to the square of the distance d (ST09, see Eq. 1 there):

$$N = \left(\frac{L}{10^{39} \text{ erg/s}} \right) \left(\frac{10 \text{ kpc}}{d} \right)^2 \quad (2)$$

This encompasses an important property of our model. Namely, using this model one can correctly evaluate normalization of the original “seed” component, which is presumably a correct \dot{M} indicator (Seifina & Titarchuk 2011). In its turn

$$L = \frac{GM_{BH}\dot{M}}{R_*} = \eta(r_*)\dot{m}L_{Ed} \quad (3)$$

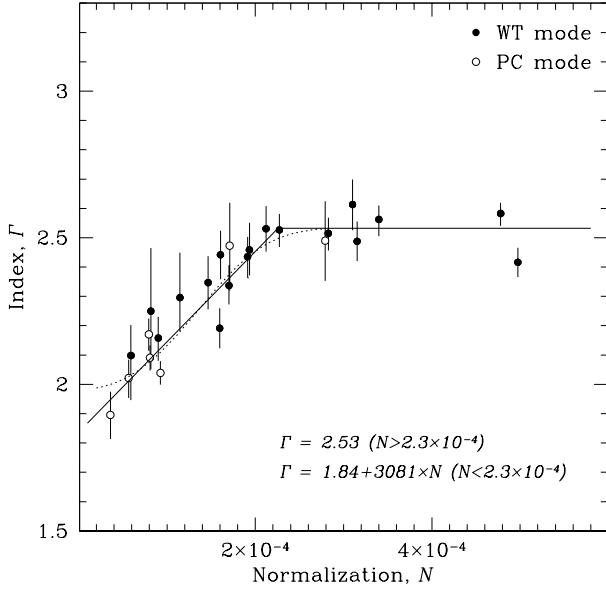


Figure 2. Γ vs N (normalization, proportional to the mass accretion rate) correlations those for OJ 287 (target source). We use a specific function for $\Gamma = 1.80 + 3.190 \times N$ for $N < 2.3 \times 10^{-4}$ and $\Gamma = 2.53$ for $N > 2.3 \times 10^{-4}$ to fit the data. Dotted curve represents best-fit model shape of Eq. 1.

Here $R_* = r_* R_S$ is an effective radius where the main energy release takes place in the disk, $R_S = 2GM/c^2$ is the Schwarzschild radius, $\eta = 1/(2r_*)$, $\dot{m} = \dot{M}/\dot{M}_{crit}$ is the dimensionless \dot{M} in units of the critical mass accretion rate $\dot{M}_{crit} = L_{Ed}/c^2$, and L_{Ed} is the Eddington luminosity.

For the formulation of the Comptonization problem, one can see Titarchuk et al. (1997); Titarchuk & Zannias (1998); Laurent & Titarchuk (1999); Borozdin et al. (1999); Shaposhnikov & Titarchuk (2009).

Spectral analysis of the *Swift*/XRT data of OJ 287, in principle, provides a general picture of the spectral evolution. We can trace the change in the spectrum shape during the IS–HSS transition in Fig. 1, which demonstrates two representative $E * F_E$ spectral diagrams for different states of OJ 287. The emergent spectra (see Fig. 1) can be described as a sum of the low energy blackbody and its fraction convolved with the Comptonization Green function (CGF) [see Eqs. (16) and (B5) in Sunyaev & Titarchuk (1980)]. The HSS and IS spectra are characterized by a strong soft blackbody component (presumably, related to the accretion disk) and a power law (as the hard tail of the CGF), while in the LHS the Comptonization component is dominant and the blackbody component is barely seen because the innermost part of the disk is fully covered by the scattering media which has a Thomson optical depth more than 2.

Analysis of the *Swift*/XRT data fits (see Fig. 1) showed that Γ monotonically increases from 2 to 2.6, when normalization of the spectral component (or \dot{M}) increases by a factor of about 5 (see points, in Fig. 2) at the outburst rise phase (IS–HSS).

4 A BH MASS ESTIMATE

Now, we use the scaling method for a BH mass estimate (M_{OJ287}) in OJ 287. The BH mass scaling method using the $\Gamma - N$ correlation is described in detail in ST09. This method consists of (i) searching

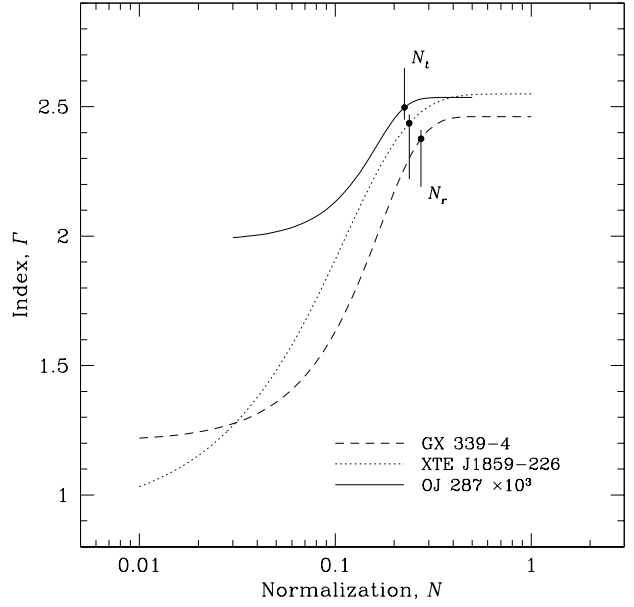


Figure 3. Γ vs. N (normalization, proportional mass accretion rate and BH mass) for OJ 287 (target source) and GX 339-4 and XTE 1859-226, the reference sources. The transition from the power line (linear shape) to the asymptotic horizontal asymptotic line occurs at $N_t = 0.23 \times 10^{-4}$ for OJ 287 and at $N_r = 0.32, 0.31$ for GX 339-4 and XTE 1859-226, respectively.

for such a pair of BHs for which the Γ correlates with increasing normalization N (which is proportional to mass accretion rate \dot{M} and a BH mass M , see ST09, Eq. (7) there) and the saturation level, Γ_{sat} are the same and (ii) calculating the scaling coefficient s_N which allows to determine a BH mass of the target object. It is worthwhile to emphasize that one needs a ratio of distances for the target and reference sources in order to estimate a BH mass using the following equation for the scaling coefficient

$$s_N = \frac{N_r}{N_t} = \frac{m_r}{m_t} \frac{d_t^2}{d_r^2} f_G \quad (4)$$

where N_r, N_t are normalizations of the spectra, $m_t = M_t/M_\odot$, $m_r = M_r/M_\odot$ are the dimensionless BH masses with respect to solar, d_t and d_r are distances to the target and reference sources, correspondingly. A geometry factor, $f_G = \cos i_r / \cos i_t$ where i_r and i_t are the disk inclinations for the reference and target sources, respectively [see ST09, Eq. (7)].

We found that XTE 1859-226 and GX 339-4 can be used as the reference sources because these sources met all aforementioned requirements to estimate a BH mass of the target source OJ 287 [see items (i) and (ii) above].

In Fig. 1 we show two types of the spectral states observed in OJ 287. The first one (in the bottom there) is a typical intermediate spectrum observed when the resulting luminosity is relatively low. We presented all emergent spectra of this source in terms of $EF(E)$ diagrams in order to estimate the resulting luminosity. In Fig. 2 we demonstrate the Γ versus N where N is presented in the units of L_{39}/d_{10}^2 (L_{39} is the source luminosity in units of 10^{39} erg/s and d_{10} is the distance to the source in units of 10 kpc). As one can see, the correlations of these sources are characterized by similar shapes and saturation levels $\Gamma_{sat} > 2.5$. In order to implement the scaling method we use an analytical approximation $F(N)$ for the $\Gamma - N$ correlation,

Table 2. BH masses and distances

Reference sources	$m_r^{(a)}$ (M_\odot)	$i_r^{(a)}$ (deg)	$d_r^{(b)}$ (kpc)	References
XTE 1859–226	$5.4^{(a)}$	~ 70	$\sim 4.2^{(b)}$	Corral-Santana et al. (2011), Hynes et al. (2002), Shaposhnikov & Titarchuk (2009)
GX 339-4	$12^{(a)}$	~ 70	$5.75 \pm 0.8^{(a)}$	Shaposhnikov & Titarchuk (2009), Hynes et al. (2003), Heida et al. (2017)
Target source	m_t (M_\odot)	$i_t^{(a)}$ (deg)	$d_t^{(b)}$ (kpc)	
OJ 287	2×10^8	50	1.037 Gpc	using XTE J1859–226 as a reference source
OJ 287	2×10^8	50	1.037 Gpc	using GX 339-4 as a reference source

(a) Dynamically and using the scaling method values of BH masses and system inclination; (b) source distance found in literature.

$$\begin{aligned} \Gamma(N) &= 1.84 + 3081 * N & \text{for } N < 2.3 \times 10^{-4} \\ \Gamma(N) &= 2.53 & \text{for } N > 2.3 \times 10^{-4} \end{aligned} \quad (5)$$

We estimated a BH mass for OJ 287 using Fig 2 of this manuscript and Figs. 3 and 9 in ST09, for GX 339-4 and XTE1859-226 respectively. Thus, we found that the Γ vs N correlations are self-similar, at least for $\Gamma > 2$, see Fig. 3 and from these correlations we could estimate N_t , N_r for OJ 287 and GX 339-4 and XTE1859-226, respectively. They are $N_t = 2.3 \times 10^{-4}$ and $N_{r,GX} = 0.27$, $N_{r,1859} = 0.24$, taken at the beginning of the Γ -saturation part (see solid points).

Thus, for GX 339-4 we obtained $s_N = N_r/N_t \sim 0.1 \times 10^4$ applying N -values: $N_r = 0.27$ and $N_t = 2.3 \times 10^{-4}$ (see Fig. 3). On the other hand, a value of a factor $f_G = \cos i_r / \cos i_t \sim 0.53$ for the target and reference sources can be obtained using inclinations $i_t = 50^\circ$ and $i_r = 70^\circ$ (see Table 2 and Hynes et al. (2003)). As a result of the estimated target mass (OJ 287), m_t we find that

$$m_t = f_G \frac{m_r d_t^2}{s_N d_r^2} \quad (6)$$

or

$$m_t \sim 2 \times 10^8 \frac{f_G}{0.53} \frac{m_r}{12} \left(\frac{d_t / 1.073 \times 10^6}{d_r / 5.75 \times 10^3} \right)^2 (s_N / 0.1 \times 10^4)^{-1} \quad (7)$$

where we use values of $d_t = 1.073$ Gpc and $d_r = 5.75$ kpc (see Table 2).

Also using the reference source XTE J1859-226 we estimate

$$m_t \sim 1.7 \times 10^8 \quad (8)$$

applying Eq. (6) if we substitute the values of $f_G = \cos i_r / \cos i_t = 0.53$, $s_N = 0.1 \times 10^4$, $d_r = 4.2$ kpc and $m_r = 5.4$ (see Table 2).

5 DISCUSSION

Valtonen et al. (2012) suggested that a BH mass of the secondary in OJ 287 is about $\sim 1.4 \times 10^8 M_\odot$ using the orbital solution. Komossa et al. (2021), hereafter KOM21 found two X-ray spectral states in OJ 287 (see Fig.4 there). Their so called 'hard state' dominated by the power law component and 'soft state' characterized by a soft component which became very strong when the source was very bright similar to those presented in Fig. 1 here. KOM21 also estimated the secondary BH mass, M_{sec} as about 1.5×10^8 if $L_x/L_{Edd} < 1.7 \times 10^{-2}$. On the other hand KOM21 claimed that the Eddington ratio L_x/L_{Edd} , that they found, surprisingly low, 5.6×10^{-4} with an assumption that $M_{BH} \sim 1.8 \times 10^{10}$ solar masses. In fact, our result confirmed their guess that L_x/L_{Edd} is on the of

order of 2×10^{-2} and thus, a BH mass is about 2×10^8 solar masses and is related to the secondary BH in the OJ 287.

Our analysis of the Fall 2016 – Spring 2017 Swift observations identified two distinct spectral states of OJ 287: the intermediate and a soft one. Those states correspond to the initial rise of the X-ray spectral index correlated to increase of the mass accretion rate (intermediate state) followed by saturation of the spectral index after reaching a certain level of accretion rate. The results of spectral analysis of the intermediate and soft states were used to estimate the value of the mass accretion rate corresponding to the saturation of the spectral index and consequently constrain the BH mass. The third spectral state of OJ 287 that can be characterized by harder source spectrum and represents a different accretion regime, was not the subject of our analysis.

6 CONCLUSIONS

The multi-wavelength outburst activity in OJ 287 with X-ray telescope (XRT) on the *Swift* call into question whether the source contains one or two black holes (BHs). It is very important to reveal the characteristics of this binary. In the presented work we demonstrated that the OJ 287 X-ray spectra underwent the state transition from the intermediate state (IS) to the high/soft state (HSS) (see Fig. 1). We found that energy spectra in all spectral states can be modeled using a product of the *tbabs* and a Comptonization component, BMC (see XSPEC). Moreover, in OJ 287 we discovered the correlation of the photon index Γ with normalization, N (proportional to the disk mass accretion rate \dot{M} , see Fig. 2) similar to those established in BH Galactic sources by ST09. We found that Γ increases monotonically with \dot{M} from the intermediate state (IS) to the high-soft state HSS, and then saturates at $\Gamma \sim 2.6$. This can be considered as observational evidence of the presence of a BH in OJ 287. Based on this correlation, we apply the scaling method (ST09) to estimate a BH mass $\sim 2 \times 10^8$ solar masses, using the well-studied X-ray BH binaries, GX 339-4 and XTE J1859-226 as reference sources (see Fig. 3).

ACKNOWLEDGEMENTS

This work made use of data supplied by the UK *Swift* Science Data Centre at the University of Leicester. The authors are grateful to Dr. Kim Page of the UK *Swift* Science Data Centre for the help with *Swift*/XRT data processing and analysis.

The authors would like to thank Sergey Sazonov, Alexey Vikhlinin and Sergey Trudolyubov for careful reading of the manuscript and valuable suggestions. We are especially grateful to Colm Elliott, Marla Kouri-Towe and Michele Delmaire for the proof reading and useful suggestions about corrections to the text of the manuscript.

DATA AVAILABILITY

The *Swift* data is available to download through the UK Swift Data Science website <https://www.swift.ac.uk/archive>.

REFERENCES

- Borozdin, K., Revnivtsev, M., Trudolyubov, S. et al., 1999, *ApJ*, 517, 367
Corral-Santana, J.M. et al. 2011 *MNRAS*, 413, L15
Gupta S. P., et al., 2012, *New Astron.*, 17, 8
Heida, J., et al. 2017, *ApJ*, 846, 132
Hynes, R.I. et al. 2002, *MNRAS*, 331, 189
Hynes, R.I. et al. 2003, *ApJ*, 583, L95
Komossa, S., et al., 2021, *MNRAS*, 504, 5575
Laurent, P., & Titarchuk, L. 2011, *ApJ*, 727, 34 (LT11)
Laurent, P., & Titarchuk, L. 1999, *ApJ*, 511, 289 (LT99)
Prince R., et al. 2021, *MNRAS*, 508, 315
Sagar R., Stalin C. S., Gopal-Krishna, Wiita P. J., 2004, *MNRAS*, 348, 176
Seifina, E., & Titarchuk, L. 2011, *ApJ*, 737, 128
Shakura, N.I., & Sunyaev, R.A. 1973, *A&A*, 24, 337 (SS73)
Shaposhnikov, N., & Titarchuk, L. 2007, *ApJ*, 663, 449 (ST07)
Shaposhnikov, N., & Titarchuk, L. 2009, *ApJ*, 699, 453 (ST09)
Sunyaev, R.A. & Titarchuk, L.G. 1980, *A&A*, 86, 121
Titarchuk, L.G., Mastichiadis, A. & Kylafis, N.D. 1997, *ApJ*, 487, 834
Titarchuk, L. & Zannias, T. 1998, *ApJ*, 499, 315
Titarchuk, L.G. & Fiorito, R. 2004, *ApJ*, 612, 988
Titarchuk, L. & Seifina, E. 2021, *MNRAS*, 501, 5659
Valtonen M. J. et al., 2006, *ApJ*, 646, 36
Valtonen M. J. et al., 2010, *Celest. Mech. Dyn. Astron.*, 106, 235
Valtonen, M., Ciprini, S. & Pihajoki, P. 2012, *MNRAS*, 427, 77 (VAL12)
Willingale, R., et al., 2013, *MNRAS*, 431, 394
Wilms, J., Allen, A., McCray, R. 2000, *ApJ*, 542, 914